Deterministic Fast Scrambling with Neutral Atom Arrays

Tomohiro Hashizume, Gregory S. Bentsen, Sebastian Weber, and Andrew J. Daley

Phys. Rev. Lett. **126**, 200603 — Published 19 May 2021

DOI: 10.1103/PhysRevLett.126.200603

Deterministic Fast Scrambling with Neutral Atom Arrays

Tomohiro Hashizume,[1,*] Gregory S. Bentsen,[2,*] Sebastian Weber,[3] and Andrew J. Daley[1]

[1] *Department of Physics and SUPA, University of Strathclyde, Glasgow G4 0NG, UK*
[2] *Martin A. Fisher School of Physics, Brandeis University, Waltham MA, USA*
[3] *Institute for Theoretical Physics III and Center for Integrated Quantum Science and Technology, University of Stuttgart, 70550 Stuttgart, Germany*

(Dated: April 13, 2021)

Fast scramblers are dynamical quantum systems that produce many-body entanglement on a timescale that grows logarithmically with the system size N. We propose and investigate a family of deterministic, fast scrambling quantum circuits realizable in near-term experiments with arrays of neutral atoms. We show that three experimental tools – nearest-neighbor Rydberg interactions, global single-qubit rotations, and shuffling operations facilitated by an auxiliary tweezer array – are sufficient to generate nonlocal interaction graphs capable of scrambling quantum information using only $\mathcal{O}(\log N)$ parallel applications of nearest-neighbor gates. These tools enable direct experimental access to fast scrambling dynamics in a highly controlled and programmable way, and can be harnessed to produce highly entangled states with varied applications.

Quantum information scrambling describes a process in which initially localized quantum information is delocalized by the dynamics of a many-body system and encoded into a many-body entangled state [1–4], thereby effectively hiding the information from local observers. This process cannot occur instantaneously: the fast scrambling conjecture states that scrambling can develop on timescales no shorter than $t_* \gtrsim \log N$ which scale logarithmically with the system size N. Systems that saturate this conjectured bound on the scrambling time t_* are known as *fast scramblers* [2]. Fast scrambling dynamics can rapidly generate Page-scrambled states, pure quantum states of a many-body system whose reduced density matrix ρ_A is maximally mixed for almost all subsystems A of size $|A| < N/2$ [1–3]. Prototypical models for fast scrambling [3, 5–9], inspired by the study of quantum information in black holes [1, 2, 10], often feature randomness and long-range couplings as key ingredients, although some recent deterministic models have been proposed with sparse or all-to-all coupling graphs with varying weights [11–13].

In this work, we propose experimental tools for achieving fast scrambling in near-term experiments with one-dimensional (1D) arrays of optically-trapped neutral atoms [14–25]. By rapidly shuffling atoms using optical tweezers it is possible to implement a broad family of nonlocal, sparsely-coupled quantum circuits that realize *fast scrambling quantum channels* [2–4]. Using such shuffling techniques for long-lived ground-state atomic qubits allows for the generation of highly non-local interaction graphs with only global rotations and nearest-neighbor Rydberg interactions. Though shuffling operations will generally be slower than Rydberg gates, limiting the number of gates to $\mathcal{O}[\log(N)]$ minimises the primary sources of noise and decoherence, which arise from laser excitations to Rydberg levels [21, 26–30]. The simplest versions of these circuits efficiently produce many-body-entangled *graph states* [31], known computational resources for measurement-based quantum computation [32, 33], quantum metrology [34], quantum error-correction [35], and quantum cryptography [36]. More sophisticated circuits built with the same experimental tools yield strongly scrambling quantum channels capable of robustly protecting quantum information against multi-qubit erasure [10, 37–39].

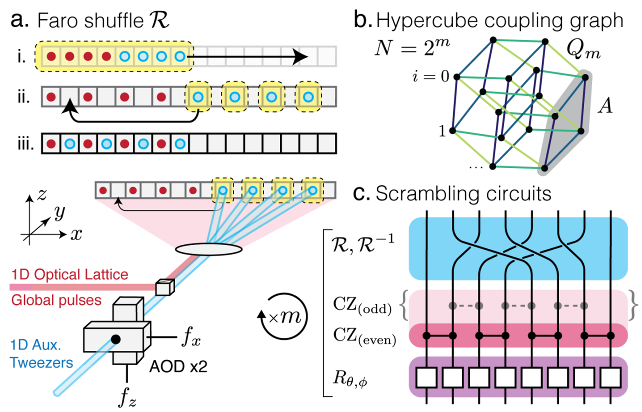

FIG. 1. **Fast scrambling via quasi-1D shuffling.** (a) Neutral atoms (red dots, blue circles) trapped in a static 1D optical lattice (gray boxes) can be rapidly rearranged via a two-step shuffling operation $\mathcal{R}$ (i-iii) facilitated by an auxiliary 1D tweezer array (bottom-left). Iterated shuffling and nearest-neighbor Rydberg interactions yield effective interactions on highly nonlocal coupling graphs such as the m-regular hypercube graph Q_m (b). More generally, circuits (c) composed of shuffles (blue), nearest-neighbor controlled-Z operations (red), and global rotations (purple) can be harnessed to generate Page-scrambled quantum states in m iterations, or strongly-scrambling quantum channels in $2m$ iterations.

Below we analyze iterated (Floquet) circuits built with these tools both for the idealised unitary case and the dissipative case expected in realistic implementations. We demonstrate that initially-separable states can be Page-scrambled using only $m \equiv \lceil \log_2 N \rceil$ nearest-neighbor interaction layers and construct deterministic circuits with only $2m$ interaction layers that strongly scramble quantum information regardless of the input state.

The basis for our protocol is the possibility to realize a family of sparse nonlocal coupling graphs via a quasi-1D shuffling procedure (Fig. 1a) on atoms in optical lattices facilitated by an auxiliary programmable 1D tweezer array. Straightforward stretching and interleaving tweezer operations [40–43] (Fig. 1a(i-iii)) can be used to rapidly shuffle the atomic positions. For $N = 8$ these motions execute the permutation

$$\mathcal{R} = \begin{pmatrix} 0 & 1 & 2 & 3 & 4 & 5 & 6 & 7 \\ 0 & 4 & 1 & 5 & 2 & 6 & 3 & 7 \end{pmatrix} \tag{1}$$

with atoms labelled by $i = 0, 1, \ldots, N-1$. More generally, for system sizes $N = 2^m$ with m an integer, a *perfect shuffle* or *Faro shuffle* operation [44, 45] executes the nonlocal mapping

$$i' = \mathcal{R}(i = b_m \ldots b_2 b_1) = b_1 b_m \ldots b_2, \tag{2}$$

which cyclically permutes the bit order of the atomic index $i = b_m \ldots b_2 b_1$ written in binary such that the least significant bit b_1 of i becomes the most significant bit of $\mathcal{R}(i)$. The shuffling operation $\mathcal{R}$, along with its inverse $\mathcal{R}^{-1}$ and generalizations thereof [46], are built on established tweezer-assisted techniques for defect-removal in atom arrays [41–43], and can be implemented rapidly using a pair of Acousto-Optic Deflectors (AOD) in crossed configuration and driven by independent RF signals f_x, f_z (Fig. 1a, bottom-left).

Repeated shuffling operations $\mathcal{R}$ dramatically rearrange the atomic positions. As a result, the propagation of quantum information is no longer constrained by the underlying 1D geometry of the fixed optical lattice. The simplest iterated circuit $\mathcal{E}_{Q_m} \equiv [\mathcal{R} \cdot \mathrm{CZ}_{(\mathrm{even})}]^m$ generates effective controlled-Z interactions on the m-regular hypercube graph Q_m [47, 48], a highly nonlocal, sparsely-connected coupling graph shown in Fig. 1b. These nonlocal couplings allow many-body entanglement to be built up rapidly and efficiently using far fewer Rydberg interaction layers than would be needed in strictly 1D systems without shuffling. For example, given $N = 2^m$ qubits initialized in the product state $\prod_i |+\rangle_i = \prod_i (|0\rangle + |1\rangle)_i/\sqrt{2}$ the circuit $\mathcal{E}_{Q_m}$ produces the Page-scrambled graph state $|Q_m\rangle$ after only m interaction layers $\mathrm{CZ}_{(\mathrm{even})}$ [34, 46].

More sophisticated circuits built using the same experimental tools (Fig. 1c) can robustly scramble quantum information irrespective of the input state. By including global Hadamard H and Phase P rotations, one can implement a *strongly-scrambling circuit*

$$\mathcal{E}_\mathrm{s} \equiv [\mathcal{R}^{-1} \cdot \mathrm{CZ}_{(\mathrm{odd})} \cdot H \cdot P]^m [\mathcal{R}^{-1} \cdot \mathrm{CZ}_{(\mathrm{even})} \cdot H \cdot P]^m \tag{3}$$

that yields widespread many-body entanglement after only $2m$ interaction layers $\mathrm{CZ}_{(\mathrm{even})}, \mathrm{CZ}_{(\mathrm{odd})}$ for arbitrary

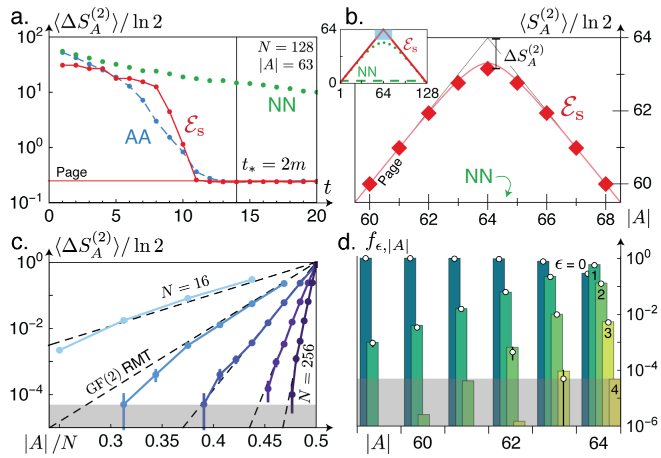

FIG. 2. **Page scrambling in $2m = 2\log_2 N$ steps.** (a) The mean deficit $\langle \Delta S_A^{(2)} \rangle$ from volume-law entanglement entropy, sampled over 2×10^4 random bipartitions $A \cup \overline{A}$ of fixed size $|A|$, decreases in the circuit $\mathcal{E}_\mathrm{s}$ on $N = 128$ qubits (solid red) at a rate comparable to a random all-to-all circuit (dashed blue) and much faster than a comparable nearest-neighbor circuit (dotted green). (b) After $2m$ circuit layers the mean Renyi entropy $\langle S_A^{(2)} \rangle$ (red diamonds), nearly saturates the Page curve (red), compared to a nearest-neighbor circuit of the same depth (b, inset). (c) The mean entropy deficit $\langle \Delta S_A^{(2)} \rangle$ agrees with random matrix theory (dotted black) to within sampling fluctuations for $N = 16, 32, 64, 128, 256$ (light to dark). (d) The fraction $f_{\epsilon,|A|}$ of subsystems A having less than maximal entanglement entropy (white dots) vanishes exponentially as a function of $\Delta S_A^{(2)}/\ln 2 = \epsilon = 0, 1, 2, 3$, in agreement with random matrix theory (vertical bars, light to dark). Error bars shown or smaller than markers; lines are guides to the eye; gray windows show statistical noise floor.

input states, as demonstrated by numerical studies of Clifford circuits (Fig. 2)[46, 49, 50]. For $N = 128$ initially z-polarized qubits, randomly-chosen subsystems A consisting of an extensive number $|A| = N/2 - 1$ of output qubits exhibit nearly maximal entanglement entropy after only $t_* = 2m = 14$ interaction layers, as measured by the Renyi entropy $S_A^{(2)} \equiv -\ln \mathrm{Tr}\left[\rho_A^2\right]$ of the reduced density matrix $\rho_A \equiv \mathrm{Tr}_{\overline{A}}[\rho]$ (Fig. 2a). The average deficit $\langle \Delta S_A^{(2)} \rangle \equiv |A| \ln 2 - \langle S_A^{(2)} \rangle$ from perfect volume-law entanglement, sampled over 2×10^4 randomly-chosen bipartitions $A \cup \overline{A}$ (solid red), rapidly decreases as a function of interaction layer t, saturating the Page limit $\Delta S_A^{(2)} = 2^{2|A|-N-1}$ (horizontal red) [1, 51] prior to layer $t_* = 2m$. The timescale $t_* \sim \log N$ required for complete scrambling is comparable to that of a random all-to-all circuit (dashed blue) – generally regarded as a prototypical fast scrambler [2, 3, 8, 12, 52] – and much shorter than for a nearest-neighbor circuit constructed without shuffling operations (dotted green).

In fact the $2m$ interaction layers of the circuit $\mathcal{E}_\mathrm{s}$ suffice to generate volume-law mean entanglement entropy

$\langle S_A^{(2)} \rangle \approx |A| \ln 2$ at all length scales $|A| < N/2$ of the output state $\rho = \mathcal{E}_\mathrm{s}[\rho_0]$. Randomly-chosen bipartitions $A \cup \overline{A}$, when organized by subsystem size $|A|$, reveal a nearly ideal Page curve [1, 51] (Fig. 2b, red). The mean entanglement deficit $\langle \Delta S_A^{(2)} \rangle$ is extremely small for almost all subsystem sizes and becomes substantial only for very large $|A| \sim N/2$. Moreover, it is in excellent agreement with the predictions of random matrix theory (RMT) for binary matrices representing random stabilizer states over a range of system sizes (Fig. 2c) [46].

The widespread delocalization of information generated by the scrambling circuit $\mathcal{E}_\mathrm{s}$ is especially apparent when one considers how unlikely it is to find a subsystem A of the output state ρ with anything less than maximal entanglement (Fig. 2d). Because the scrambling circuit $\mathcal{E}_\mathrm{s}$ consists entirely of gates chosen from the Clifford group, the Renyi entropy differs from its maximum value only by discrete bits $\Delta S_A^{(2)} / \ln 2 = \epsilon = 0, 1, 2, \ldots$ [49, 50]. We therefore count the fraction $f_{\epsilon,|A|}$ of the sampled bipartitions whose Renyi entropies differ from maximal by an amount ϵ (Fig. 2d). We find that exponentially-many subsystems A have maximal entanglement entropy $\epsilon = 0$ (for $|A| < N/2$), whereas it is exponentially rare to find a subsystem A with entropy deficit $\epsilon > 0$.

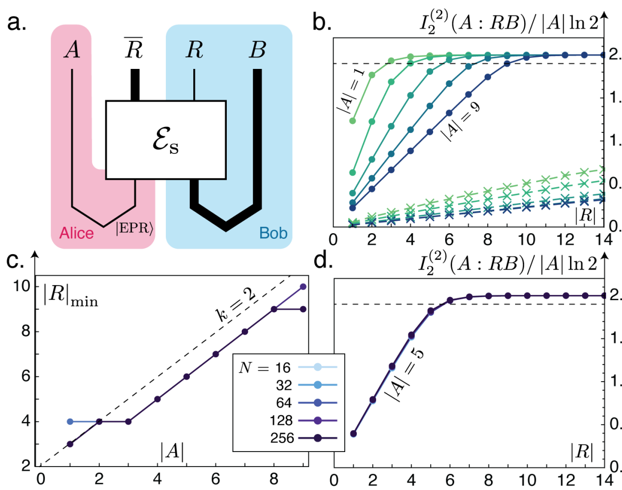

FIG. 3. **Deterministic scrambling in the Hayden-Preskill thought experiment.** (a) Scrambling in the circuit $\mathcal{E}_\mathrm{s}$ can be characterized by the mutual information $I_2^{(2)}(A : RB)$ between Alice's register A (red) and Bob's registers R, B (blue). (b) For $N = 128$ qubits, the mutual information grows rapidly as a function of Bob's output register R over a range of message sizes $|A| = 1, 3, 5, 7, 9$ (light to dark), saturating to within 5% of its maximum value (dotted black) after Bob has collected only a handful $|R|_\mathrm{min} \geq |A| + k$ of output qubits with $k \leq 2$ (c, dotted black). Nearest-neighbor circuits of the same depth (crosses, dashed lines) show relatively low mutual information by comparison. (d) At fixed $|A| = 5$, $I_2^{(2)}(A : RB)$ shows strong data collapse as a function of system size $N = 16, 32, 64, 128, 256$ (light to dark). Error bars smaller than markers; lines are guides to the eye.

Due to its ability to rapidly delocalize – and thereby conceal – quantum information, the scrambling circuit $\mathcal{E}_\mathrm{s}$ naturally serves a practical function in the context of quantum error correction and quantum communication. In particular, strongly-scrambling quantum channels are known to be excellent encoders that optimally protect quantum information against the effects of single-qubit erasure and other forms of local dissipation [10, 37, 52]. While prototypical examples of such encoding circuits are usually random, we demonstrate here that our deterministic circuit $\mathcal{E}_\mathrm{s}$ can be leveraged for precisely the same task, as illustrated by the thought experiment of Hayden and Preskill [10, 37–39] (Fig. 3). Here, quantum information held by a local observer Alice A is dumped into the strongly scrambling quantum channel $\mathcal{E}_\mathrm{s}$ and is subsequently recovered with high fidelity by a maximally-entangled observer Bob after measuring only a small subset R of the output qubits and neglecting the rest $\overline{R}$. High fidelity teleportation of Alice's quantum information to Bob's register B occurs if and only if the unitary channel is strongly scrambling [10, 38] and therefore presents a sharp criterion for diagnosing the presence of scrambling dynamics in our circuit $\mathcal{E}_\mathrm{s}$.

From the perspective of quantum error correction, we view the scrambling circuit $\mathcal{E}_\mathrm{s}$ as an encoding circuit that optimally protects Alice's information against erasure, allowing Bob to successfully reconstruct Alice's state even after discarding the large majority of output qubits $\overline{R}$. This is guaranteed in principle by large bipartite mutual information

$$I_2^{(2)}(A : RB) = S_A^{(2)} + S_{RB}^{(2)} - S_{ARB}^{(2)} \tag{4}$$

between the qubits A in Alice's control and those R, B in Bob's control (Fig. 3a). Numerical calculations with Clifford circuits demonstrate that the circuit $\mathcal{E}_\mathrm{s}$ on $N = 128$ qubits performs quite well as an encoding channel: the mutual information increases linearly with the number of output qubits $|R|$ collected by Bob (Fig. 3b) and rapidly saturates to within 5% of its maximum value $I_2^{(2)}(A : RB) = 2\,|A| \ln 2$ after he has collected a few more than $|A|$ qubits. Physically, this implies that Bob need only gather a few $|R|_\mathrm{min} \geq |A| + k$ of the output qubits in order to successfully decode Alice's message (Fig. 3c), with $k \leq 2$ for large N. By contrast, nearest-neighbor circuits of the same depth (Fig. 3b, dashed lines) show low mutual information over a large range of output qubits $|R|$. For fixed message size $|A| = 5$, the mutual information shows strong data collapse as a function of system size N (Fig. 3d), indicating robustness to finite-size effects.

The numerical evidence presented in Figs. 2, 3 demonstrates that $\mathcal{E}_\mathrm{s}$ is a fast scrambler in the ideal unitary case. Any realistic implementation of this scrambling circuit, however, must contend with the effects of noise and dissipation that will inevitably degrade its performance. In the following, we analyze a possible experimental realization of $\mathcal{E}_s$ in detail including the effects of decoherence to characterize its scrambling properties in a realistic setup.

We propose to use long-lived ground states $|0\rangle, |1\rangle$ of neutral atoms as qubit states [30, 53, 54]. Single-qubit rotations allow for implementation of Hadamard and Phase gates. By exciting $|1\rangle$ to a Rydberg state, controlled-Z gates between neighboring atoms can be realized using strong van der Waals interactions [21, 26–29, 55–57]. Current experiments already achieve Rydberg gate fidelities > 0.99 [21, 57]. A primary advantage of these operations is that they may be applied in parallel, using global optical or RF pulses. For our simulations, we take into account crosstalk between atoms separated by the distance r, resulting from the $1/r^6$-decay of the van der Waals interaction. We model decoherence as dephasing noise with error rate p per atom after each interaction layer [46].

To distinguish between scrambling and decoherence, we attempt to recover Alice's information using a probabilistic decoding circuit (Fig. 4a, dotted purple), following the scheme of Yoshida, Kitaev, and Yao [37–39]. This decoder consists of a complex-conjugated copy of the scrambling circuit and the ability to measure EPR pairs; decoding protocols of this type have been realized in pioneering experiments with trapped ions [58]. In the unitary case $p = 0$, the circuit decodes Alice's quantum information with a fidelity $F_{\text{EPR}} = 2^{I_2^{(2)}(A:RB)-2|A|}$, conditioned on successful detection of $|R|$ EPR pairs by Bob with probability $P_{\text{EPR}} = 2^{-I_2^{(2)}(A:RB)}$ (Fig. 4b). Bob's ability to recover Alice's information is degraded by decoherence $p > 0$, where the product $\delta \equiv P_{\text{EPR}} F_{\text{EPR}} 2^{2|A|} \leq 1$ gives a natural metric for the strength of decoherence [38, 39].

We compare the scrambling circuit to an analogous circuit without shuffling and thus with controlled-Z gates between nearest neighbors only. Notably, the nearest-neighbor circuit requires a longer time, measured in the number of interaction layers, to accomplish scrambling. While the decoherence metric δ behaves the same for the nearest neighbor circuit and the scrambling circuit $\mathcal{E}_s$ (Fig. 4d), for $p > 0$, the reachable teleportation fidelity F_{EPR} is significantly smaller for the slow scrambling nearest neighbor circuit (Fig. 4c). This demonstrates that fast scrambling is crucial in non-error-corrected systems, precisely because fewer gates provide fewer opportunities for dissipation. Our scrambling circuit $\mathcal{E}_s$ is optimal in this regard as it generates strong scrambling using the minimal number of interaction layers $2m \sim \mathcal{O}(\log N)$ allowed by the fast scrambling conjecture [2, 3, 8].

We have shown how deterministic, highly-nonlocal iterated (Floquet) circuits can generate fast scrambling dynamics in a way that is amenable to direct experimental realization using fast shuffle operations on neutral atom qubits. This technique allows for rapid long-range

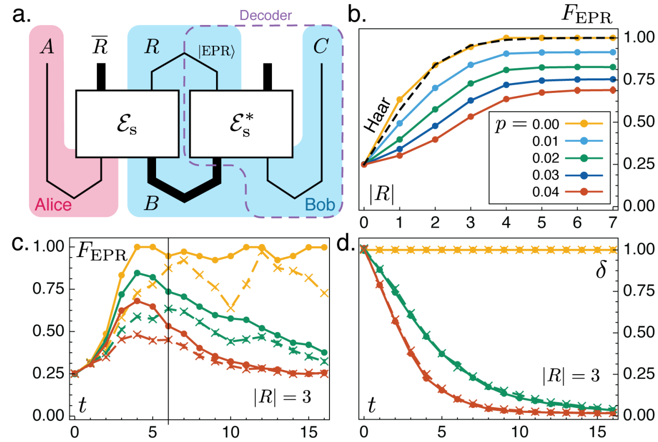

FIG. 4. **Information scrambling in the presence of dissipation.** (a) Scrambling in the circuit $\mathcal{E}_s$ is diagnosed by the fidelity F_{EPR} of recovering Alice's quantum information A on Bob's register C using a probabilistic decoding circuit (dotted purple). (b) For $N = 8$ at fixed circuit depth $t = 6$ the fidelity grows with the number of qubits $|R|$ used in the decoder, indicating successful teleportation of Alice's information with fidelity $> 50\%$ even in the presence of single-qubit errors at rates $p = 0.00, 0.01, \ldots, 0.04$ per two-qubit gate (light to dark). For $p = 0$ the fidelity is nearly identical to that of a Haar-random circuit (dotted black). (c) The fidelity (dots, solid lines) grows with circuit depth t, and substantially outperforms nearest-neighbor circuits of the same depth (crosses, dotted lines) in the presence of dissipation. (d) The dissipation parameter δ falls as a function of circuit depth in both the scrambling circuit and nearest-neighbor circuit. Each datapoint averaged over 6×10^4 quantum trajectories, with error bars smaller than markers; lines are guides to the eye.

spreading of entanglement while minimising errors from excitation of atoms to Rydberg states, and uses only shuffling operations, global single-qubit rotations and parallel nearest-neighbor interactions. Building fast scrambling circuits in the laboratory opens connections to a wide range of ongoing areas, including fundamental limits on the spreading of quantum information [2, 3, 8, 59], experimental studies of toy models of black holes [11, 60–63], efficient encoders for quantum error-correcting codes [10], and highly-entangled resources for quantum computation [32, 33]. While we simulate example cases with stabilizer states [49, 50, 64] for large system sizes, analogous circuits built in the laboratory may employ arbitrary quantum rotations, exploring the complete many-body Hilbert space. We note that these graphs might also be constructed by other means, including collisional gate implementations for neutral atoms, or via direct wiring of hypercubic coupling graphs in superconducting qubit systems.

In the final stages of this work, we became aware of a proposal [63] for further explorations of many-body quantum teleportation, based around nearest-neighbor

Rydberg models with scrambling times $t_* \propto N$. The protocols we describe here for fast scrambling could be immediately combined with these interesting proposals to extend the example from Fig. 4 discussed here.

We thank Jon Pritchard, Monika Schleier-Smith, Hans Peter Büchler, and Simon Evered for stimulating and helpful discussions. GSB is supported by the DOE GeoFlow program (DE-SC0019380). Work at the University of Strathclyde was supported by the EPSRC Programme Grant DesOEQ (EP/P009565/1), the EPSRC Quantum Technologies Hub for Quantum Computing and simulation (EP/T001062/1), the European Unions Horizon 2020 research and innovation program under grant agreement No. 817482 PASQuanS, and AFOSR grant number FA9550-18-1-0064. SW was supported by the European Union under the ERC consolidator grant SIRPOL (grant N. 681208).

* These authors contributed equally to this work.

[1] D. N. Page, Average entropy of a subsystem, Phys. Rev. Lett. **71**, 1291 (1993).
[2] Y. Sekino and L. Susskind, Fast scramblers, J. High Energy Phys. **2008**, 065.
[3] N. Lashkari, D. Stanford, M. Hastings, T. Osborne, and P. Hayden, Towards the fast scrambling conjecture, J. High Energ. Phys. **2013**, 22.
[4] P. Hosur, X.-L. Qi, D. A. Roberts, and B. Yoshida, Chaos in quantum channels, J. High Energ. Phys. **2016**, 4.
[5] J. Ye, S. Sachdev, and N. Read, Solvable spin glass of quantum rotors, Phys. Rev. Lett. **70**, 4011 (1993).
[6] A. Kitaev, A simple model of quantum holography (2015), Part 1 and Part 2.
[7] J. Maldacena and D. Stanford, Remarks on the sachdev-ye-kitaev model, Phys. Rev. D **94**, 106002 (2016).
[8] G. Bentsen, Y. Gu, and A. Lucas, Fast scrambling on sparse graphs, Proc Natl Acad Sci USA **116**, 6689 (2019).
[9] L. Piroli, C. Sünderhauf, and X.-L. Qi, A random unitary circuit model for black hole evaporation, Journal of High Energy Physics **2020**, 1 (2020).
[10] P. Hayden and J. Preskill, Black holes as mirrors: quantum information in random subsystems, J. High Energy Phys. **2007**, 120.
[11] G. Bentsen, T. Hashizume, A. S. Buyskikh, E. J. Davis, A. J. Daley, S. S. Gubser, and M. Schleier-Smith, Treelike interactions and fast scrambling with cold atoms, Phys. Rev. Lett. **123**, 130601 (2019).
[12] R. Belyansky, P. Bienias, Y. A. Kharkov, A. V. Gorshkov, and B. Swingle, Minimal model for fast scrambling, Phys. Rev. Lett. **125**, 130601 (2020).
[13] Z. Li, S. Choudhury, and W. V. Liu, Fast scrambling without appealing to holographic duality, Physical Review Research **2**, 043399 (2020).
[14] D. Weiss, J. Vala, A. Thapliyal, S. Myrgren, U. Vazirani, and K. Whaley, Another way to approach zero entropy for a finite system of atoms, Phys. Rev. A **70**, 040302 (2004).
[15] J. Yang, X. He, R. Guo, P. Xu, K. Wang, C. Sheng, M. Liu, J. Wang, A. Derevianko, and M. Zhan, Coherence preservation of a single neutral atom qubit transferred between magic-intensity optical traps, Physical review letters **117**, 123201 (2016).
[16] H. Kim, W. Lee, H.-g. Lee, H. Jo, Y. Song, and J. Ahn, In situ single-atom array synthesis using dynamic holographic optical tweezers, Nat Commun **7**, 1 (2016).
[17] C. Gross and I. Bloch, Quantum simulations with ultracold atoms in optical lattices, Science **357**, 995 (2017).
[18] H. Bernien, S. Schwartz, A. Keesling, H. Levine, A. Omran, H. Pichler, S. Choi, A. S. Zibrov, M. Endres, M. Greiner, V. Vuleti, and M. D. Lukin, Probing many-body dynamics on a 51-atom quantum simulator, Nature **551**, 579 (2017).
[19] J. Zhang, G. Pagano, P. Hess, A. Kyprianidis, P. Becker, H. Kaplan, A. Gorshkov, Z.-X. Gong, and C. Monroe, Observation of a many-body dynamical phase transition with a 53-qubit quantum simulator, Nature **551**, 601 (2017).
[20] H. Levine, A. Keesling, A. Omran, H. Bernien, S. Schwartz, A. S. Zibrov, M. Endres, M. Greiner, V. Vuleti, and M. D. Lukin, High-fidelity control and entanglement of rydberg-atom qubits, Phys. Rev. Lett. **121**, 123603 (2018).
[21] H. Levine, A. Keesling, G. Semeghini, A. Omran, T. T. Wang, S. Ebadi, H. Bernien, M. Greiner, V. Vuleti, H. Pichler, and M. D. Lukin, Parallel implementation of high-fidelity multiqubit gates with neutral atoms, Phys. Rev. Lett. **123**, 170503 (2019).
[22] M. Kim, Y. Song, J. Kim, and J. Ahn, Quantum ising hamiltonian programming in trio, quartet, and sextet qubit systems, PRX Quantum **1**, 020323 (2020).
[23] P. Scholl, M. Schuler, H. J. Williams, A. A. Eberharter, D. Barredo, K.-N. Schymik, V. Lienhard, L.-P. Henry, T. C. Lang, T. Lahaye, *et al.*, Programmable quantum simulation of 2d antiferromagnets with hundreds of rydberg atoms, arXiv:2012.12268 (2020).
[24] S. Ebadi, T. T. Wang, H. Levine, A. Keesling, G. Semeghini, A. Omran, D. Bluvstein, R. Samajdar, H. Pichler, W. W. Ho, S. Choi, S. Sachdev, M. Greiner, V. Vuletic, and M. D. Lukin, Quantum phases of matter on a 256-atom programmable quantum simulator, arXiv:2012.12281 (2020).
[25] A. W. Young, W. J. Eckner, W. R. Milner, D. Kedar, M. A. Norcia, E. Oelker, N. Schine, J. Ye, and A. M. Kaufman, Half-minute-scale atomic coherence and high relative stability in a tweezer clock, Nature **588**, 408 (2020).
[26] M. Lukin, M. Fleischhauer, R. Cote, L. Duan, D. Jaksch, J. Cirac, and P. Zoller, Dipole blockade and quantum information processing in mesoscopic atomic ensembles, Phys. Rev. Lett. **87**, 037901 (2001).
[27] R. Heidemann, U. Raitzsch, V. Bendkowsky, B. Butscher, R. Lw, L. Santos, and T. Pfau, Evidence for coherent collective rydberg excitation in the strong blockade regime, Phys. Rev. Lett. **99**, 163601 (2007).
[28] D. Jaksch, J. Cirac, P. Zoller, S. Rolston, R. Ct, and M. Lukin, Fast quantum gates for neutral atoms, Phys. Rev. Lett. **85**, 2208 (2000).
[29] M. M. Mller, M. Murphy, S. Montangero, T. Calarco, P. Grangier, and A. Browaeys, Implementation of an experimentally feasible controlled-phase gate on two blockaded rydberg atoms, Phys. Rev. A **89**, 032334 (2014).
[30] M. Saffman, T. Walker, and K. Mlmer, Quantum information with rydberg atoms, Rev. Mod. Phys. **82**, 2313

(2010).
[31] M. Hein, W. Dür, J. Eisert, R. Raussendorf, M. Nest, and H.-J. Briegel, Entanglement in graph states and its applications, arXiv:quant-ph/0602096 (2006).
[32] R. Raussendorf and H. J. Briegel, A one-way quantum computer, Phys. Rev. Lett. **86**, 5188 (2001).
[33] R. Raussendorf, D. E. Browne, and H. J. Briegel, Measurement-based quantum computation on cluster states, Phys. Rev. A **68**, 022312 (2003).
[34] N. Shettell and D. Markham, Graph states as a resource for quantum metrology, Phys. Rev. Lett. **124**, 110502 (2020).
[35] S. Y. Looi, L. Yu, V. Gheorghiu, and R. B. Griffiths, Quantum-error-correcting codes using qudit graph states, Phys. Rev. A **78**, 042303 (2008).
[36] K. Chen and H.-K. Lo, Multi-partite quantum cryptographic protocols with noisy ghz states, arXiv:quant-ph/0404133 (2004).
[37] B. Yoshida and A. Kitaev, Efficient decoding for the hayden-preskill protocol, arXiv:1710.03363 (2017).
[38] B. Yoshida and N. Y. Yao, Disentangling scrambling and decoherence via quantum teleportation, Phys. Rev. X **9**, 011006 (2019).
[39] N. Bao and Y. Kikuchi, Hayden-Preskill decoding from noisy Hawking radiation, J. High Energ. Phys. **2021**, 1.
[40] J. Beugnon, C. Tuchendler, H. Marion, A. Gatan, Y. Miroshnychenko, Y. R. Sortais, A. M. Lance, M. P. Jones, G. Messin, A. Browaeys, and P. Grangier, Two-dimensional transport and transfer of a single atomic qubit in optical tweezers, Nature Phys **3**, 696 (2007).
[41] M. Endres, H. Bernien, A. Keesling, H. Levine, E. R. Anschuetz, A. Krajenbrink, C. Senko, V. Vuletic, M. Greiner, and M. D. Lukin, Atom-by-atom assembly of defect-free one-dimensional cold atom arrays, Science **354**, 1024 (2016).
[42] D. Barredo, S. de Lsleuc, V. Lienhard, T. Lahaye, and A. Browaeys, An atom-by-atom assembler of defect-free arbitrary two-dimensional atomic arrays, Science **354**, 1021 (2016).
[43] D. Barredo, V. Lienhard, S. de Lsleuc, T. Lahaye, and A. Browaeys, Synthetic three-dimensional atomic structures assembled atom by atom, Nature **561**, 79 (2018).
[44] P. Diaconis, R. Graham, and W. M. Kantor, The mathematics of perfect shuffles, Adv. Appl. Math. **4**, 175 (1983).
[45] D. Aldous and P. Diaconis, Shuffling cards and stopping times, Amer. Math. Monthly **93**, 333 (1986).
[46] See Supplemental Material at [URL will be inserted by publisher] for supporting derivations and additional experimental details.
[47] D. B. West *et al.*, *Introduction to graph theory*, Vol. 2 (Prentice hall Upper Saddle River, 2001).
[48] B. Bollobás, *Modern graph theory*, Vol. 184 (Springer Science and Business Media, 2013).
[49] D. Gottesman, The heisenberg representation of quantum computers, arXiv:quant-ph/9807006 (1998).
[50] S. Aaronson and D. Gottesman, Improved simulation of stabilizer circuits, Phys. Rev. A **70**, 052328 (2004).
[51] E. Bianchi and P. Don, Typical entanglement entropy in the presence of a center: Page curve and its variance, Phys. Rev. D **100**, 105010 (2019).
[52] M. J. Gullans and D. A. Huse, Dynamical purification phase transition induced by quantum measurements, Phys. Rev. X **10**, 041020 (2020).
[53] L. Henriet, L. Beguin, A. Signoles, T. Lahaye, A. Browaeys, G.-O. Reymond, and C. Jurczak, Quantum computing with neutral atoms, Quantum **4**, 327 (2020).
[54] M. Morgado and S. Whitlock, Quantum simulation and computing with rydberg qubits, arXiv:2011.03031 (2020).
[55] L. Theis, F. Motzoi, F. Wilhelm, and M. Saffman, High-fidelity rydberg-blockade entangling gate using shaped, analytic pulses, Phys. Rev. A **94**, 032306 (2016).
[56] L. Isenhower, E. Urban, X. Zhang, A. Gill, T. Henage, T. A. Johnson, T. Walker, and M. Saffman, Demonstration of a neutral atom controlled-not quantum gate, Phys. Rev. Lett. **104**, 010503 (2010).
[57] I. S. Madjarov, J. P. Covey, A. L. Shaw, J. Choi, A. Kale, A. Cooper, H. Pichler, V. Schkolnik, J. R. Williams, and M. Endres, High-fidelity entanglement and detection of alkaline-earth rydberg atoms, Nat. Phys. **16**, 857 (2020).
[58] K. Landsman, C. Figgatt, T. Schuster, N. Linke, B. Yoshida, N. Yao, and C. Monroe, Verified quantum information scrambling, Nature **567**, 61 (2019).
[59] M. B. Hastings and T. Koma, Spectral gap and exponential decay of correlations, Commun. Math. Phys. **265**, 781 (2006).
[60] D. I. Pikulin and M. Franz, Black hole on a chip: Proposal for a physical realization of the sachdev-ye-kitaev model in a solid-state system, Phys. Rev. X **7**, 031006 (2017).
[61] A. Chew, A. Essin, and J. Alicea, Approximating the sachdev-ye-kitaev model with majorana wires, Phys. Rev. B **96**, 121119 (2017).
[62] I. Danshita, M. Hanada, and M. Tezuka, Creating and probing the sachdev–ye–kitaev model with ultracold gases: Towards experimental studies of quantum gravity, Progress of Theoretical and Experimental Physics **2017**, 083I01 (2017).
[63] T. Schuster, B. Kobrin, P. Gao, I. Cong, E. T. Khabiboulline, N. M. Linke, M. D. Lukin, C. Monroe, B. Yoshida, and N. Y. Yao, Many-body quantum teleportation via operator spreading in the traversable wormhole protocol, arXiv:2102.00010 (2021).
[64] J. Iaconis, Quantum state complexity in computationally tractable quantum circuits, PRX Quantum **2**, 010329 (2021).
[65] M. A. Nielsen and I. L. Chuang, *Quantum Computation and Quantum Information*, 10th ed. (Cambridge University Press, Cambridge, 2010).
[66] P. Selinger, Generators and relations for n-qubit clifford operators, Log.Meth.Comput.Sci. **11**, 80 (2015).
[67] A. Nahum, J. Ruhman, S. Vijay, and J. Haah, Quantum Entanglement Growth under Random Unitary Dynamics, Physical Review X **7**, 031016 (2017).
[68] V. Kolchin, *Random Graphs*, Encyclopedia of Mathematics and its Applications (Cambridge University Press, Cambridge, 1998).
[69] G. H. Hardy and E. M. Wright, *An Introduction to the Theory of Numbers*, 4th ed. (Oxford University Press, Oxford, 1975).
[70] H. Abraham and *et al*, Qiskit: An open-source framework for quantum computing (2019).